Research Square

Preprints are preliminary reports that have not undergone peer review.
They should not be considered conclusive, used to inform clinical practice,
or referenced by the media as validated information.

Glucose infusion rate and gut microbiota maturation in NICU neonates

Hiroya Ogita
Kagawa University
Sonoko Kondo
ijichi.sonoko@kagawa-u.ac.jp

Kagawa University
Takeo Kondo
Kagawa University
Katsufumi Nishioka
Kagawa University
Kota Inoue
Kagawa University
Aya Morimoto
Kagawa University
Hirosuke Morita
Kagawa University
Shinji Nakamura
Jichi Medical School
Kosuke Koyano
Kagawa University
Haruyuki Nakayama-Imaohji
Kagawa University
Tomomi Kuwahara
Kagawa University
Takashi Kusaka
Kagawa University

Article

Keywords:

Posted Date: November 12th, 2026

DOI: https://doi.org/10.21203/rs.3.rs-11122756/v1

License: This work is licensed under a Creative Commons Attribution 4.0 International License.
Read Full License

Additional Declarations:
No competing interests reported.

Table 1 is available in the Supplementary Files section.

Glucose infusion rate and gut microbiota maturation in NICU neonates

Hiroya Ogita[1], Sonoko Kondo[1,*], Takeo Kondo[1], Katsufumi Nishioka[1], Kota Inoue[1], Aya Morimoto[1], Hirosuke Morita[1], Shinji Nakamura[2], Kosuke Koyano[1], Haruyuki Nakayama-Imaohji[3], Tomomi Kuwahara[3], Takashi Kusaka[1]

[1]Department of Pediatrics, Faculty of Medicine, Kagawa University, Kita-gun, Kagawa, Japan

[2]Department of Pediatrics, Faculty of Medicine, Jichi Medical School, Shimotsuke, Tochigi, Japan

[3]Department of Microbiology, Faculty of Medicine, Kagawa University, Kita-gun, Kagawa, Japan

Corresponding Author: Sonoko Kondo, MD, PhD

Department of Pediatrics, Faculty of Medicine, Kagawa University

1750-1 Ikenobe, Miki-cho, Kita-gun, Kagawa 761-0793, Japan

Tel: +81-87-891-2171; Fax: +81-87-891-2172

Email: ijichi.sonoko@kagawa-u.ac.jp

Short title:

GIR and Gut Microbiota in NICU Neonates

Abstract

Background

The neonatal gut microbiota undergoes rapid maturation and is shaped by multiple clinical factors. Although the glucose infusion rate (GIR) is essential for preventing neonatal hypoglycemia, its impact on early gut microbiota development remains unclear.

Methods

A longitudinal observational study of 10 neonatal intensive care unit (NICU) neonates was conducted. Stool samples were collected daily until postnatal day 14 and analyzed by 16S rRNA gene sequencing. Neonates were stratified into Low- and High-GIR groups (<6.0 vs. ≥6.0 mg/kg/min, respectively). Microbial diversity, taxonomic composition, functional predictions, and Random Forest models were compared.

Results

Ninety stool samples were analyzed. The High-GIR group showed greater cumulative glucose exposure, lower α-diversity, and a distinct β-diversity trajectory. The Low-GIR group was enriched in *Streptococcus* and Enterobacteriaceae, whereas the high-GIR group was dominated by Staphylococcaceae, Enterococcaceae, and *Bifidobacterium*. Functional prediction indicated accelerated microbial maturation in the Low-GIR group, with the enrichment of vitamin K2, B vitamin, and short-chain fatty acid biosynthesis pathways. A Random Forest model accurately classified both groups.

Conclusions

Higher intravenous glucose exposure was associated with delayed taxonomic and functional maturation of the neonatal gut microbiota, including reduced microbial vitamin biosynthesis, suggesting a link between early metabolic management and microbial development.

Introduction

The neonatal gut microbiota plays a central role in immune development and metabolic homeostasis, with lasting effects on host health[1]. Early microbial colonization is highly dynamic and shaped by multiple perinatal factors. The mode of delivery is a key determinant of initial microbial exposure, e.g., vaginally delivered infants acquire maternal vaginal microbiota, including *Lactobacillus* and Actinobacteria (recently renamed Actinomycetota), whereas cesarean delivery is associated with reduced microbial load and decreased Bacteroidetes (Bacteroidota) diversity[2,3]. Feeding practices further influence microbial development, with breastfeeding promoting the expansion of commensal bacteria[4]. In addition, even short-term antibiotic exposure disrupts normal microbial maturation[5]. Furthermore, factors affecting the function of gut microbiota, such as vitamin K metabolism, may also influence microbial development. Neonates are predisposed to vitamin K deficiency due to the immature microbial production of menaquinone, which may be exacerbated further by antibiotic exposure[6,7].

In healthy neonates, the gut microbiota undergoes rapid expansion during the first weeks of life. The most pronounced shift occurs within the first week, with a transition from Proteobacteria (Pseudomonadota) dominance to Firmicutes (Bacillota) and Actinobacteria (Actinomycetota) dominance alongside increased α-diversity[8]. However, these findings are largely derived from rooming-in term infants and may not be generalizable to neonates requiring intensive care.

In preterm infants, the gut microbiota develops within the constrained environment of the neonatal intensive care unit (NICU), where reduced diversity and Pseudomonadota-dominant profiles are commonly observed[9,10]. Microbial succession follows a characteristic trajectory that is influenced by clinical interventions, and even brief antibiotic exposure can disrupt this maturation and impair the development of short-chain fatty acid-producing bacteria[11].

Additionally, nutritional management in the NICU significantly influences microbial development. In older pediatric patients with intestinal failure receiving parenteral nutrition, dysbiosis characterized by reduced diversity, decreased short-chain fatty acid production, and increased abundance of potentially pathogenic taxa has been reported[12]. Similarly, in NICU infants, total parenteral nutrition is associated with reduced microbial diversity and delayed colonization by *Bacteroides* and *Bifidobacterium*[13].

In neonatal intensive care, particularly in preterm infants at high risk for hypoglycemia, intravenous glucose is administered to avoid neurological sequelae until stable enteral feeding is established. The maximum glucose infusion rate (GIR) required during this period serves as a comprehensive clinical surrogate for neonatal immaturity, severity of illness, and delayed transition to enteral autonomy. Although fluctuations of blood glucose levels are considered a physiological adaptation, we hypothesized that a prolonged reliance on high intravenous glucose would be strongly linked with a distinct trajectory of microbial development, characterized by delayed taxonomic and functional maturation, including impaired short-chain fatty acid production and vitamin biosynthesis.

To our knowledge, no previous study has performed daily longitudinal sampling from birth to characterize the gut microbiota of term and preterm infants during the early neonatal period. Therefore, this study aimed to elucidate the temporal dynamics of gut microbiota development using daily stool samples collected from birth to postnatal day 14, and to examine its association with cumulative GIR exposure in NICU neonates. Furthermore, we sought to determine whether specific early microbial signatures could reliably predict this high-GIR clinical phenotype using machine learning approaches.

Methods

Patient selection

This was a single-center, prospective observational study conducted in the NICU at Kagawa University Hospital between August 2023 and October 2023. All participants received routine care as determined by the attending physicians. Clinical data, including diagnoses, treatments, daily nutritional intake, medications, and laboratory data were recorded. Notably, eight of the ten participants received antibiotic therapy during the study period. Eligible participants met the following inclusion criteria: (1) admission to our NICU within 24 h of birth and (2) written informed consent obtained from a parent or legal guardian. Neonates were excluded if they had: (1) a major congenital anomaly, e.g., critical congenital heart disease or gastrointestinal atresia; (2) a condition directly affecting glucose metabolism, e.g., inborn errors of metabolism; (3) other severe comorbidities; or (4) insufficient clinical information available during the study period.

Sample collection and processing

Whenever feasible, stool samples were collected once daily from spontaneously passed stools in the neonate's diapers, from the day of birth until postnatal day 14. Immediately after defecation, the diapers were placed in sealed containers. These containers were collected daily, maintained at room temperature, and delivered to the research coordinator. All samples were processed within 24 h of collection.

Each sample was assigned a coded identifier linked to the postnatal day of collection and relevant daily clinical variables, e.g., GIR, enteral feeding volume, and antibiotic exposure. The samples were analyzed in an anonymized manner ensuring that individual participants could not be identified.

DNA preparation

Stool samples (0.1 g/mL in phosphate-buffered saline) were centrifuged at 12,000 × *g* for 5 min to collect the bacterial cells. The resulting pellets were washed with phosphate-buffered saline and subsequently resuspended in Tris-EDTA buffer. For 16S rRNA gene sequencing, DNA was extracted using a NucleoSpin DNA Stool Kit (MACHEREY-NAGEL, Düren, Germany). DNA concentrations were quantified using a Qubit dsDNA BR Assay Kit (Thermo Fisher Scientific, Waltham, MA, USA).

16S rRNA gene analysis

Sequencing libraries were prepared by amplifying the V3-V4 hypervariable region of the 16S rRNA gene using the 341F and 805R primer set, as reported previously[14]. The libraries were sequenced on an Illumina MiSeq platform (Illumina, Inc., San Diego, CA, USA) using the Miseq Reagent Lit V3 (600 Cycles) to generate 301-bp paired-end reads. The final library was prepared at 12 pM with a 20% ΦX spike-in. Sequence denoising and the generation of amplicon sequence variants were performed using the DADA2 plugin within QIIME2. Taxonomic assignment of the resulting amplicon sequence variants was conducted using a pre-trained Naïve Bayes classifier based on the SILVA database (release 138).

Microbial diversity and taxonomic analysis

To evaluate gut microbiota diversity, α- and β-diversity metrics were calculated. α-Diversity was assessed by calculating the observed features and Shannon, Simpson, and Chao1 indices as measures of species richness and evenness within each sample. β-Diversity was evaluated by constructing Bray-Curtis dissimilarity matrices to assess differences in overall microbial community composition and was visualized using principal coordinates analysis. The temporal trajectories of these diversity metrics were compared between the

Low- and High-GIR groups, which were defined according to the maximum GIR required during the observation period. For taxonomic comparisons, a linear discriminant analysis effect size (LEfSe) algorithm was employed to identify biologically meaningful bacterial taxa characterizing the Low- and High-GIR groups. In LEfSe analysis, predefined thresholds, specifically a logarithmic linear discriminant analysis score cutoff of 3.0 and a *p*-value of <0.05, were applied to focus on biologically meaningful differences, and the results were visualized using a volcano plot.

Predictive functional profiling

To predict the functional metabolic potential of the neonatal gut microbiota, the Phylogenetic Investigation of Communities by Reconstruction of Unobserved States 2 (PICRUSt2) pipeline was utilized. The analysis was executed using the representative sequences and feature tables derived from the 16S rRNA amplicon sequencing data as input, generating predicted abundance profiles of MetaCyc metabolic pathways for each sample. The resulting profile data were subjected to downstream statistical analyses, and specific functional enrichment was evaluated by calculating the $\log_2$ fold change between the Low- and High-GIR groups.

Machine learning and predictive modeling

A machine learning algorithm using a Random Forest classifier was applied to construct a predictive model capable of distinguishing the high-GIR clinical phenotype based on early taxonomic profiles. During model construction, variable importance was evaluated quantitatively based on the Mean Decrease in Gini impurity. Predictive accuracy was subsequently optimized through feature selection, evaluating sequential subsets to identify a minimal target panel of top-ranked predictive variables. The diagnostic performance of the

optimized models was assessed using receiver operating characteristic analysis, and the area under the curve (AUC) was calculated.

Statistical analysis

All statistical analyses and graphical representations were performed within the R software environment (version 4.4.2). Microbiome data processing and diversity calculations were conducted using the phyloseq (version 1.50.0) and MicrobiotaProcess (version 1.18.0) packages. β-Diversity distances were calculated utilizing the vegan package (version 2.7-2). Machine learning modeling and receiver operating characteristic analyses were performed using the randomForest (version 4.7-1.2) and pROC (version 1.19.0.1) packages, respectively. For intergroup comparisons of clinical background characteristics, the Mann-Whitney *U* test was applied for continuous variables with a non-normal distribution, while Fisher's exact test was used for categorical variables. Cumulative GIR exposure over the 14-day period was quantified by calculating the AUC for each neonate. Given the longitudinal nature of the daily sampling protocol, differences in α-diversity indices between the Low- and High-GIR groups were evaluated using repeated-measures analysis to account for intra-subject correlation across the 14-day observation period. Similarly, structural differences in β-diversity trajectories were statistically evaluated by repeated-measures permutational multivariate analysis of variance (9,999 permutations) using the adonis function, with permutations strictly stratified by individual neonates. For all analyses, a two-sided *p*-value of <0.05 was considered statistically significant. Where appropriate, false discovery rate correction was applied to address multiple comparisons.

Ethical considerations

This study was approved by the Institutional Review Board of Kagawa University

(approval no. 2023-020) and was conducted in accordance with the Declaration of Helsinki. Prior to enrollment, parents or legal guardians were provided with a detailed explanation of the study objectives, procedures, anticipated benefits and risks, and the plans for data anonymization and dissemination. Written informed consent was obtained from the parents or legal guardians of all enrolled neonates. All data were strictly anonymized prior to analysis.

Results

Clinical characteristics of the study cohort

During the study period, 10 neonates admitted to our NICU met the inclusion criteria, did not meet any of the exclusion criteria, and had stool samples collected daily between postnatal days 0 and 14. A total of 90 stool samples were obtained from the 10 neonates, and 16S rRNA gene sequencing was performed on all samples. On the basis of the maximum GIR during the observation period, six neonates were classified into the Low-GIR group (maximum GIR < 6.0 mg/kg/min) and four were classified into the High-GIR group (maximum GIR ≥ 6.0 mg/kg/min).

There were no significant differences between the groups in terms of sex, gestational age, birth weight, mode of delivery, postnatal day of enteral feeding initiation, neonatal antibiotic exposure, or maternal factors (tocolytic use, antibiotic use, and gestational diabetes mellitus) (Table 1). In contrast, the postnatal day of formula feeding initiation was significantly delayed in the High-GIR group compared with the Low-GIR group (median, 10.0 vs. 5.0 days, respectively; $p = 0.017$). By the nature of the study design, the maximum GIR was significantly higher in the High-GIR group than in the Low-GIR group (median [range], 8.5 [7.2–9.5] vs. 4.85 [4.5–5.1] mg/kg/min, respectively; $p < 0.001$). To confirm that the binary classification based on the maximum GIR accurately reflected the total glucose exposure, the cumulative GIR exposure was calculated as the AUC from the daily longitudinal trajectories. The cumulative GIR AUC was significantly higher in the High-GIR group than in the Low-GIR group (Fig. 1a, b).

Gut microbial diversity is associated with the GIR

Temporal changes in the gut microbiome were assessed from postnatal day 0 to 14. α-Diversity indices were used to evaluate microbial richness and evenness (Fig. 2a). In

repeated-measures analysis, the Low-GIR group showed consistently higher observed features ($p < 0.05$) and Shannon index values ($p < 0.01$) than the High-GIR group. Chao1 and Simpson indices also demonstrated a trend toward higher values in the Low-GIR group than in the High-GIR group, although these did not reach statistical significance. Overall, α-diversity was significantly higher in the Low-GIR group than in the High-GIR group during the early neonatal period.

β-Diversity was assessed using Bray-Curtis dissimilarity and visualized by principal coordinates analysis (Fig. 2b). Group differences were tested using permutational multivariate analysis of variance with permutations stratified by individual neonates, demonstrating a significant difference in overall community composition trajectories between the Low- and High-GIR groups ($p = 0.0014$).

Taxonomic signatures characterizing the GIR-associated phenotypes

To identify specific taxa associated with the distinct microbial trajectories between both groups, LEfSe analysis was performed and visualized using a volcano plot (Fig. 3). In the Low-GIR group, LEfSe analysis identified the significant enrichment of Pseudomonadota (class Gammaproteobacteria) and Enterobacterales/Enterobacteriaceae, including the genera *Klebsiella* and *Streptococcus*. Conversely, the High-GIR group was characterized by the enrichment of Bacillota (class Bacillus), Bacillales, and the families Staphylococcaceae, Enterococcaceae, as well as Bifidobacteriales/Bifidobacteriaceae (including the genus *Bifidobacterium*).

Functional maturation and vitamin biosynthesis pathways

To investigate whether these taxonomic differences translate into functional alterations, PICRUSt2 was utilized to predict the metabolic capacity of the gut microbiota (Figs. 4, S1).

Functional prediction revealed the profound enrichment of *de novo* vitamin biosynthesis pathways in the Low-GIR group (Fig. 4). Specifically, multiple pathways responsible for the synthesis of vitamin K2 (menaquinone and dimethylmenaquinol), as well as essential B vitamins including thiamin (B1), NAD (B3), pyridoxal 5′-phosphate (B6), and biotin (B7), were significantly upregulated. Furthermore, pathways associated with advanced carbohydrate degradation and short-chain fatty acid production, notably L-1,2-propanediol degradation (a precursor pathway from propionate), were enriched in the Low-GIR microbiota.

In contrast, the High-GIR group was functionally characterized by early-stage, simple carbohydrate metabolism, exhibiting a significant upregulation in lactose and galactose degradation, the *Bifidobacterium* shunt, and heterolactic fermentation (Fig. S1b). These results indicate that a prolonged reliance on a high GIR is associated with a functional delay in the anaerobic and metabolic maturation of the neonatal gut microbiome.

Identification of predictive biomarkers using machine learning

Finally, a Random Forest machine learning approach was employed to identify the key predictive features distinguishing the two clinical phenotypes and to evaluate their discriminatory power (Figs. 5, S2). Feature selection optimization demonstrated that model performance plateaued using a minimal subset of the top 5 to 10 predictive taxa (Fig. S2). Receiver operating characteristic curve analysis confirmed that a target panel consisting of these top genera, i.e., *Streptococcus*, *Enterobacteriaceae*_UKG, *Enterococcus*, *Bifidobacterium*, and *Staphylococcus*, achieved an extremely high discrimination accuracy, with an AUC of 0.965 (Fig. 5a, b). This indicates that the differential abundance of a small specific group of bacteria strongly characterizes the clinical phenotype requiring high intravenous glucose support.

Discussion

In this study, we longitudinally characterized the development of gut microbiota in NICU neonates using stool samples collected daily from birth until postnatal day 14 and examined its association with the GIR. We identified several principal findings. First, neonates requiring a higher cumulative GIR exhibited significantly lower α-diversity than those receiving a lower GIR. Second, the taxonomic and functional maturation trajectory, specifically the establishment of anaerobic metabolism and vitamin biosynthesis, was markedly attenuated in the High-GIR group. Finally, a machine learning approach identified a minimal microbial signature that highly predicted this specific clinical phenotype. These findings suggest that the functional maturation of the neonatal gut microbiota is closely associated with early postnatal nutritional autonomy and a reliance on intravenous glucose.

The reduced α-diversity observed in the High-GIR group is consistent with previous studies linking parenteral nutrition and limited enteral feeding to decreased microbial diversity. In NICU infants, total parenteral nutrition is associated with lower Shannon diversity and delayed colonization by key commensal taxa such as *Bacteroides* and *Bifidobacterium*[13]. Similarly, studies in older children with intestinal failure have demonstrated an inverse relationship between the proportion of parenteral nutrition and microbial diversity[12]. Since a higher GIR generally reflects a greater reliance on intravenous glucose and delayed advancement of enteral feeding, our findings extend these observations by demonstrating that even quantitative differences in early glucose load are intimately associated with reduced microbial diversity during the very early neonatal period.

Crucially, our functional predictions using PICRUSt2 provided mechanistic insights into the taxonomic shift identified by LEfSe analysis. As hypothesized, the microbiota in the Low-GIR group demonstrated a profound enrichment in *de novo* vitamin biosynthesis pathways, particularly vitamin K2 (menaquinone) and essential B vitamins. Neonates are

301 inherently susceptible to vitamin K deficiency bleeding due to limited placental transfer and
302 immature microbial production[6,7]. Similarly, several B vitamins are essential for energy
303 metabolism and are synthesized by the intestinal microbiota. Therefore, the reduced
304 metabolism of vitamins B1, B3, B6, and B7 in the High-GIR group may reflect metabolic
305 immaturity and delayed postnatal microbial maturation[15-18]. Our findings further suggest that
306 a prolonged reliance on high-concentration intravenous glucose, associated with a delayed
307 transition to enteral feeding, may delay intestinal microbial maturation and thereby reduce the
308 microbial contribution to host vitamin availability.
309 Furthermore, we demonstrated that the functional transition toward an obligate
310 anaerobic ecosystem was attenuated in infants exposed to a higher GIR. During normal
311 neonatal development, the gut microbiota undergoes a transition from oxygen-tolerant
312 facultative anaerobes to obligate anaerobes as intestinal oxygen tension decreases and
313 microbial ecosystems mature. Disruption of this transition has been reported in association
314 with antibiotic exposure and NICU-related interventions[9,10]. Our PICRUSt2 analysis revealed
315 that the Low-GIR group exhibited enriched pathways for complex carbohydrate degradation
316 and short-chain fatty acid precursors, e.g., L-1,2-propanediol degradation, whereas the High-
317 GIR group was dominated by simple early-stage carbohydrate metabolism, e.g., lactose
318 degradation and heterolactic fermentation. The relative predominance of taxa such as
319 Staphylococcaceae in the High-GIR group supports the notion that the ecological progression
320 toward a mature, anaerobic, short-chain fatty acid-producing microbiome was delayed. One
321 plausible explanation is that insufficient enteral substrate delivery limits the establishment of
322 these anaerobic niches.
323 Our findings also raise the possibility that the development of the gut microbiota is
324 intimately linked to metabolic adaptation in early life. In neonatal intensive care, fluctuations
325 in blood glucose levels and the requirement for intravenous glucose are observed until stable

enteral feeding is achieved. Although, such instability is considered a normal physiological adaptation, it is highly plausible that concurrent changes in the gut microbiota and the dynamic maturation of glucose metabolism are interrelated. To evaluate this clinical link further, we applied a Random Forest machine learning model. A minimal target panel of top predictive genera, which comprised low-GIR enriched taxa, e.g., *Streptococcus* and *Enterobacteriaceae*_UKG, and high-GIR enriched taxa, e.g., *Enterococcus* and *Bifidobacterium*, distinguished between the two clinical phenotypes with exceptional accuracy (AUC = 0.965). While not a direct diagnostic tool, this high predictive accuracy highlights that the high-GIR clinical state is tightly linked to a highly specific and reproducible dysbiotic signature. Neonates with a lower GIR, who are more likely to have enteral feeding established earlier, may develop a more favorable intestinal environment for microbiota maturation, whereas a higher GIR reflects delayed enteral adaptation and a persistently immature microbial ecosystem. While strict causal relationships cannot be established in the present study, these findings strongly suggest a potential link between microbial development and glucose management during this critical period.

This study has several limitations that should be considered. First, the sample size was small and derived from a single center, limiting statistical power and generalizability. Second, the GIR may reflect not only glucose load but also clinical factors such as illness severity and feeding tolerance, introducing potential confounding. While causal relationships cannot be strictly established, the GIR serves as a robust comprehensive surrogate for delayed nutritional adaptation. Third, although we utilized PICRUSt2 for functional prediction, we did not perform direct metabolomic or meta-transcriptomic analyses to confirm actual *in vivo* metabolite production. Fourth, the machine learning model was evaluated internally; strict external validation in an independent cohort is required to establish the generalization of the predictive microbial panel.

In conclusion, the present study identified distinct GIR-associated alterations in the taxonomic and functional development of the gut microbiota during the very early neonatal period. Neonates with a lower GIR, who received earlier enteral feeding, rapidly developed a gut environment conducive to anaerobic maturation and vitamin biosynthesis by postnatal day 14. Longitudinal daily stool microbiota analysis provided a powerful approach for elucidating the relationship between microbial development and early neonatal metabolic management. These findings highlight a clinical link between the functional maturation of the gut microbiota and glucose management in NICU neonates, providing important implications for optimizing early nutritional strategies.

Data availability statement

The 16S rRNA gene sequencing data have been deposited in the DNA Data Bank of Japan (accession numbers: DRR1081147-DRR1081236).

References

1. Milani C, Duranti S, Bottacini F, Casey E, Turroni F, Mahony J. et al. The first microbial colonizers of the human gut: composition, activities, and health implications of the infant gut microbiota. *Microbiol. Mol. Biol. Rev*. 2017; 81: e00036-17.
2. Dominguez-Bello MG, Costello EK, Contreras M, Magris M, Hidalgo G, Fierer N. et al. Delivery mode shapes the acquisition and structure of the initial microbiota across multiple body habitats in newborns. *Proc. Natl. Acad. Sci. U. S. A*. 2010; 107: 11971–11975.
3. Jakobsson HE, Abrahamsson TR, Jenmalm MC, Harris K, Quince C, Jernberg C. et al. Decreased gut microbiota diversity, delayed Bacteroidetes colonisation and reduced Th1 responses in infants delivered by caesarean section. *Gut* 2014; 63: 559–566.
4. Pannaraj PS, Li F, Cerini C, Bender JM, Yang S, Rollie A. et al. Association between breast milk bacterial communities and establishment and development of the infant gut microbiome. J*AMA Pediatr*. 2017; 171: 647–654.
5. Xu Y, Milburn O, Beiersdorfer T, Du L, Akinbi H, Haslam DB. Antibiotic exposure prevents acquisition of beneficial metabolic functions in the preterm infant gut microbiome. *Microbiome* 2022; 10: 103.
6. Araki S, Shirahata A. Vitamin K deficiency bleeding in infancy. *Nutrients* 2020; 212: 780.
7. Ellis JL, Wang M, Fu X, Fields CJ, Donovan SM, Booth SL. Feeding practice and delivery mode are determinants of vitamin K in the infant gut: an exploratory analysis. *Curr. Dev. Nutr*. 2022; 6: nzac019.
8. Wang XA, Li JP, Lee MS, Yang SF, Chang YS, Chen L. et al. A common trajectory of gut microbiome development during the first month in healthy neonates with limited inter-individual environmental variations. *Sci. Rep*. 2024; 14: 3264.

9. La Rosa PS, Warner BB, Zhou Y, Weinstock GM, Sodergren E, Hall-Moore CM. et al. Patterned progression of bacterial populations in the premature infant gut. *Proc. Natl. Acad. Sci. U. S. A*. 2014; 111: 12522–12527.
10. Cong X, Xu W, Janton S, Henderson WA, Matson A, McGrath JM. et al. Gut microbiome developmental patterns in early life of preterm infants: impacts of feeding and gender. *PLoS One* 2016; 11: e0152751.
11. Xu Y, Milburn O, Beiersdorfer T, Du L, Akinbi H, Haslam DB. Antibiotic exposure prevents acquisition of beneficial metabolic functions in the preterm infant gut microbiome. *Microbiome* 2022; 10: 103.
12. Neelis EG, de Koning BAE, Hulst JM, Papadopoulou R, Kerbiriou C, Rings EHHMN. et al. Gut microbiota and its diet-related activity in children with intestinal failure receiving long-term parenteral nutrition. *JPEN J. Parenter. Enteral. Nutr*. 2022; 46: 693–708.
13. Dahlgren AF, Pan A, Lam V, Gouthro KC, Simpson PM, Salzman NH. et al. Longitudinal changes in the gut microbiome of infants on total parenteral nutrition. *Pediatr. Res*. 2019; 86: 107–114.
14. Klindworth A, Pruesse E, Schweer T, Peplies J, Quast C, Horn M. et al. Evaluation of general 16S ribosomal RNA gene PCR primers for classical and next-generation sequencing-based diversity studies. *Nucleic Acids Res*. 2013; 41: e1.
15. Mascolo E. &Vernì F. Vitamin B6 and diabetes: relationship and molecular mechanisms. *Int. J. Mol. Sci*. 2020; 21: 3669.
16. Hossain, K. S., Amarasena, S. & Mayengbam, S. B vitamins and their roles in gut health. *Microorganisms* 2022; 10: 1168.
17. Yoshii K, Hosomi K, Sawane K, Kunisawa J. Metabolism of dietary and microbial vitamin B family in the regulation of host immunity. *Front. Nutr*. 2019; 6: 48.
18. Perry, C. A. & Butterick, T. A. Biotin. *Adv. Nutr*. 2024; 15: 100251.

Acknowledgments

We are thankful to Mina Aiba and Kyoko Horiuchi for their technical assistance.

Funding

This study was supported by Japan Society for the Promotion of Science (JSPS) KAKENHI Grant Numbers 24K14726 and 23K28020.

Author contributions

Ogita H, Kondo S, Kusaka T and Kuwahara T conceptualized and designed this study. Kondo T, Nishioka K, Inoue K, Morimoto A, Morita H, Nakamura S and Koyano K collected the samples. Nakayama-Imaohji H, Nakamura S and Koyano K extracted the DNA, analyzed metagenomic data and conducted statistical analyses. Ogita H, Kondo S, Kusaka T, Nakayama-Imaohji H and Kuwahara T interpreted results and wrote the manuscript.

Competing interests

The authors declare no competing interests.

Consent statement

Written informed consent was obtained from the parents of the patients in this study.

Figure legends

Fig. 1: Daily GIR trajectories and cumulative glucose exposure from birth to postnatal day 14.

a Longitudinal changes in the daily GIR (mg/kg/min) for each neonate during the 14-day observation period. Dots represent individual daily measurements. The solid lines indicate the smoothed trajectories fitted by a generalized linear model (cubic polynomial), with the shaded areas representing the 95% confidence intervals. Neonates with a maximum GIR of <6.0 mg/kg/min during the observation period were classified into the Low-GIR group (blue), whereas those with a maximum GIR of ≥6.0 mg/kg/min were classified into the High-GIR group (red). **b** Comparison of cumulative GIR exposure over 14 days, calculated as the AUC, between the High- and Low-GIR groups. The box plots show the median and interquartile ranges, with individual data points overlaid. Statistical significance was determined using the Mann-Whitney *U* test (*$p < 0.05$). Abbreviations: AUC, area under the curve; GIR, glucose infusion rate; maxGIR, maximum glucose infusion rate.

Fig. 2: Gut microbial diversity and community composition associated with the GIR during the first 14 postnatal days.

a α-Diversity indices (observed features, Chao1, Shannon, and Simpson) compared between the High-GIR (H, red) and Low-GIR (L, blue) groups. Data are visualized as violin plots with overlaid box plots representing the median and interquartile ranges, along with individual sample points. Statistical differences between the groups were evaluated using repeated-measures analysis to account for daily longitudinal sampling within individual neonates (*$p < 0.05$, **$p < 0.01$). **b** PCoA plot based on Bray-Curtis dissimilarity evaluating β-diversity. Each point represents a single daily stool sample, color-coded by group (red: High-GIR; blue: Low-GIR). The ellipses represent the 95% confidence intervals for each group. The statistical

significance of differences in overall microbial community trajectories was determined using RM-PERMANOVA with permutations stratified by individual neonates ($p = 0.0014$).
Abbreviations: GIR, glucose infusion rate; maxGIR, maximum glucose infusion rate; PCoA, principal coordinates analysis; RM-PERMANOVA, repeated-measures permutational multivariate analysis of variance.

Fig. 3: Taxonomic signatures differentiating the High- and Low-GIR groups.
Volcano plot visualizing the results of LEfSe analysis. The *x*-axis displays the signed LDA score (coefficient), and the *y*-axis displays the -$\log_{10}$-transformed *p*-value. Taxa significantly enriched in the Low-GIR group (signed LDA score ≤ -3.0 and $p < 0.05$) are positioned on the left, while those significantly enriched in the High-GIR group (signed LDA score ≥ 3.0 and $p < 0.05$) are positioned on the right. The color gradient of the significant dots corresponds to the prevalence of each taxon within its respective group (blue gradient: Low-GIR group; red gradient: High-GIR group). The size of each dot represents the mean relative abundance of the taxon. Semi-transparent gray dots indicate taxa that did not meet the threshold for statistical significance or effect size. Dashed lines indicate the threshold cutoffs ($p = 0.05$ and |LDA score| = 3.0). Abbreviations: GIR, glucose infusion rate; LDA, linear discriminant analysis; LEfSe, linear discriminant analysis effect size.

Fig. 4: Predicted functional metabolic pathways significantly enriched in the Low-GIR microbiota.
Dot plot visualizing the top 20 metabolic pathways significantly upregulated in the Low-GIR group compared with the High-GIR group, as predicted by PICRUSt2 analysis based on 16S rRNA gene sequences. The *y*-axis displays the identified MetaCyc functional pathways. The *x*-axis represents the $\log_2$ fold change (Low-GIR [L] / High-GIR [H]). The size of each dot is

proportional to the statistical significance (-$\log_{10}$ *p*-value). The color gradient corresponds to the magnitude of the $\log_2$ fold change, with darker red indicating a stronger enrichment in the Low-GIR group. The profoundly enriched pathways highlight advanced functional maturation, including the *de novo* biosynthesis of essential vitamins, e.g., menaquinone (vitamin K2), biotin, thiamin, and pyridoxal 5′-phosphate, and short-chain fatty acid precursors. Abbreviations: FC, fold change; GIR, glucose infusion rate; maxGIR, maximum glucose infusion rate.

Fig. 5: Identification of predictive microbial signatures for GIR dependence using a Random Forest machine learning model.

a ROC curves evaluating the diagnostic performance of the Random Forest classifier in distinguishing between the High (H)- and Low (L)-GIR clinical phenotypes. The plot compares three feature sets: a full model utilizing all available genera (green line, AUC = 0.950), a target panel utilizing the top 10 predictive genera (blue line, AUC = 0.965), and a minimal panel comprising only the top five predictive genera (red line, AUC = 0.965). Shaded regions indicate the 95% confidence intervals for each curve. **b** Bar chart displaying the top 10 most discriminatory taxonomic features (the target panel) identified by the model, ranked by their predictive importance (Mean Decrease Gini). The length of each bar represents the contribution of the taxon to the model's classification accuracy. Bars are color-coded based on the group in which the respective taxon is relatively enriched (red: enriched in the Low-GIR group; blue: enriched in the High-GIR group). Abbreviations: AUC, area under the curve; GIR, glucose infusion rate; maxGIR, maximum glucose infusion rate; ROC, receiver operating characteristic.

Fig. 1

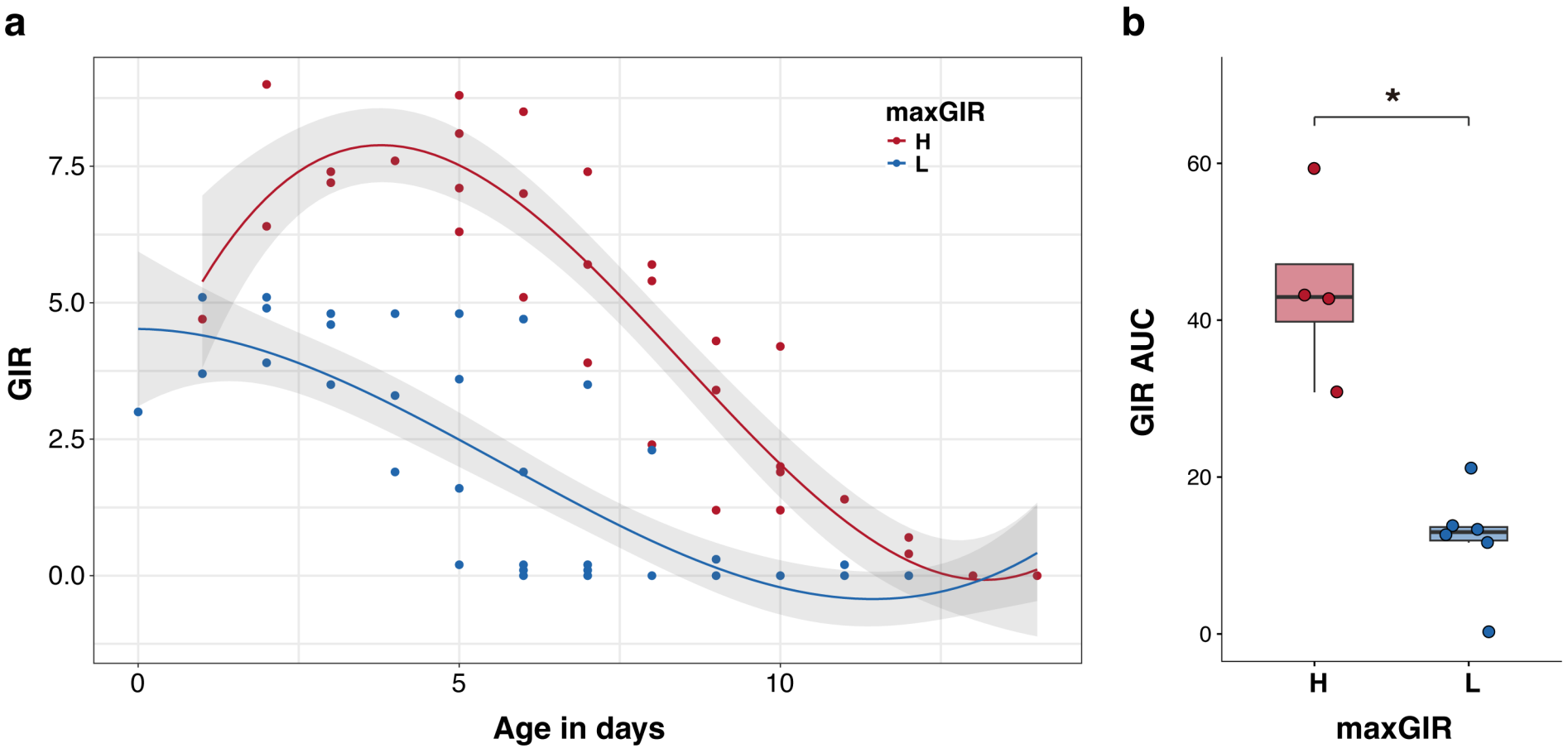

a
GIR
7.5
5.0
2.5
0.0
0
5
10
Age in days
maxGIR
H
L
b
GIR AUC
60
40
20
0
*
H
L
maxGIR

Fig. 2

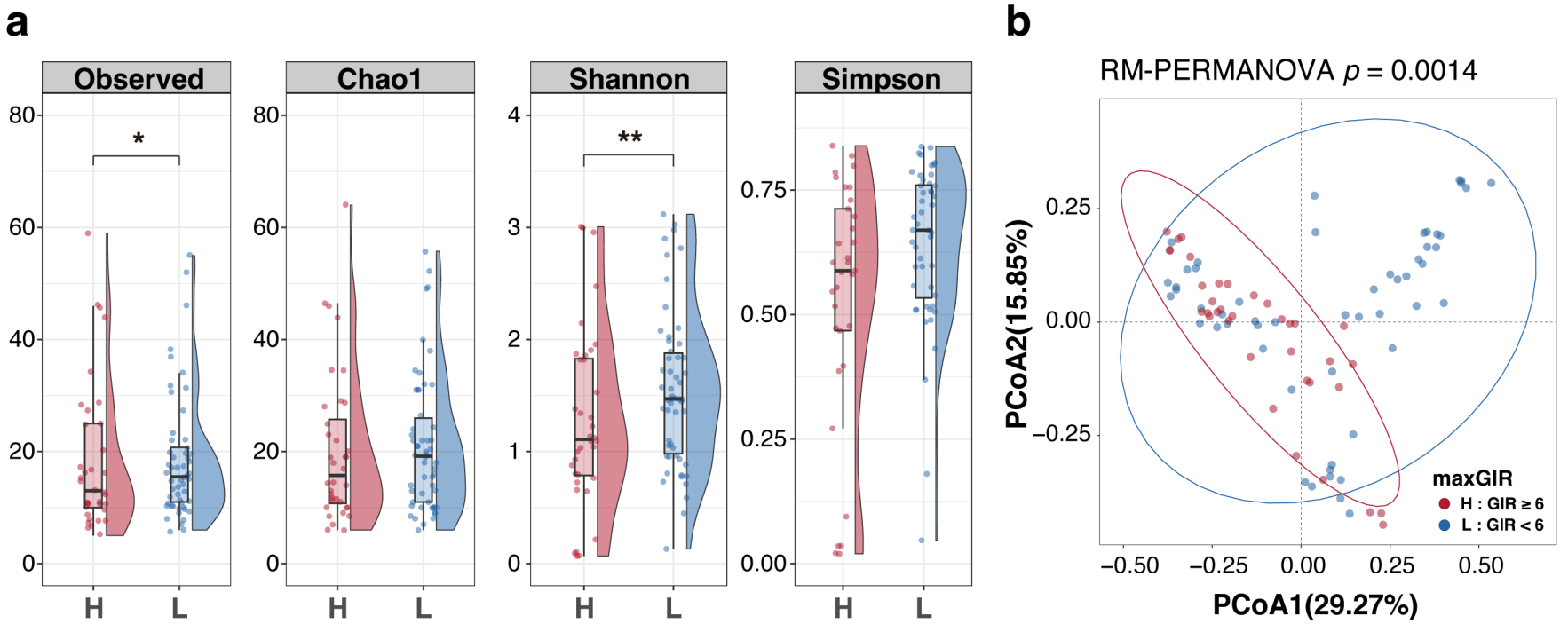

a
Observed
Chao1
Shannon
Simpson
*
**
H
L
b
RM-PERMANOVA p = 0.0014
PCoA2(15.85%)
PCoA1(29.27%)
maxGIR
H : GIR ≥ 6
L : GIR < 6

Fig. 3

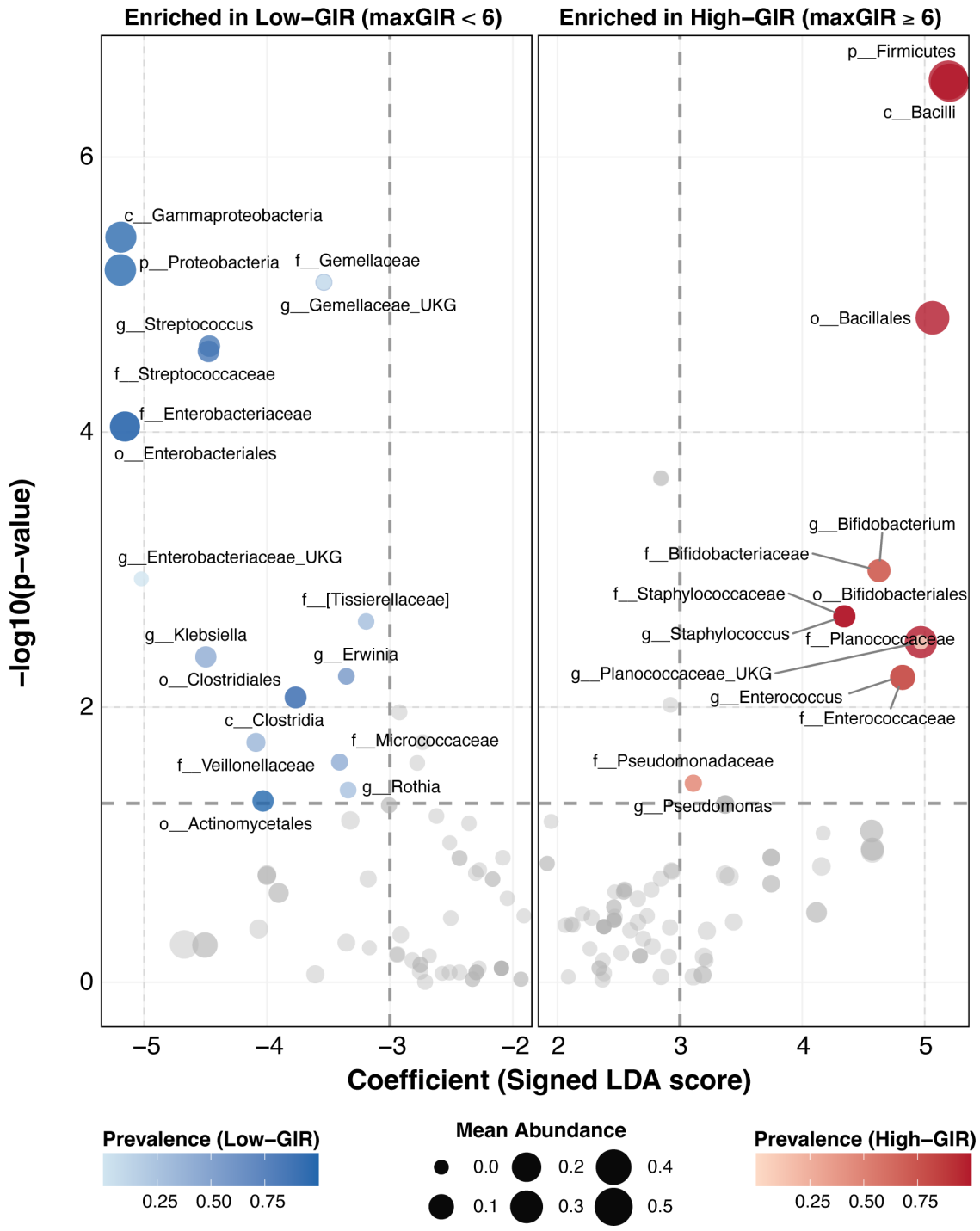

Enriched in Low−GIR (maxGIR < 6)
Enriched in High−GIR (maxGIR ≥ 6)
−log10(p−value)
Coefficient (Signed LDA score)
c__Gammaproteobacteria
p__Proteobacteria
f__Gemellaceae
g__Gemellaceae_UKG
g__Streptococcus
f__Streptococcaceae
f__Enterobacteriaceae
o__Enterobacteriales
g__Enterobacteriaceae_UKG
f__[Tissierellaceae]
g__Klebsiella
g__Erwinia
o__Clostridiales
c__Clostridia
f__Micrococcaceae
f__Veillonellaceae
g__Rothia
o__Actinomycetales
p__Firmicutes
c__Bacilli
o__Bacillales
g__Bifidobacterium
f__Bifidobacteriaceae
f__Staphylococcaceae
o__Bifidobacteriales
g__Staphylococcus
f__Planococcaceae
g__Planococcaceae_UKG
g__Enterococcus
f__Enterococcaceae
f__Pseudomonadaceae
g__Pseudomonas
Prevalence (Low−GIR)
0.25 0.50 0.75
Mean Abundance
0.0 0.2 0.4
0.1 0.3 0.5
Prevalence (High−GIR)
0.25 0.50 0.75

Fig. 4

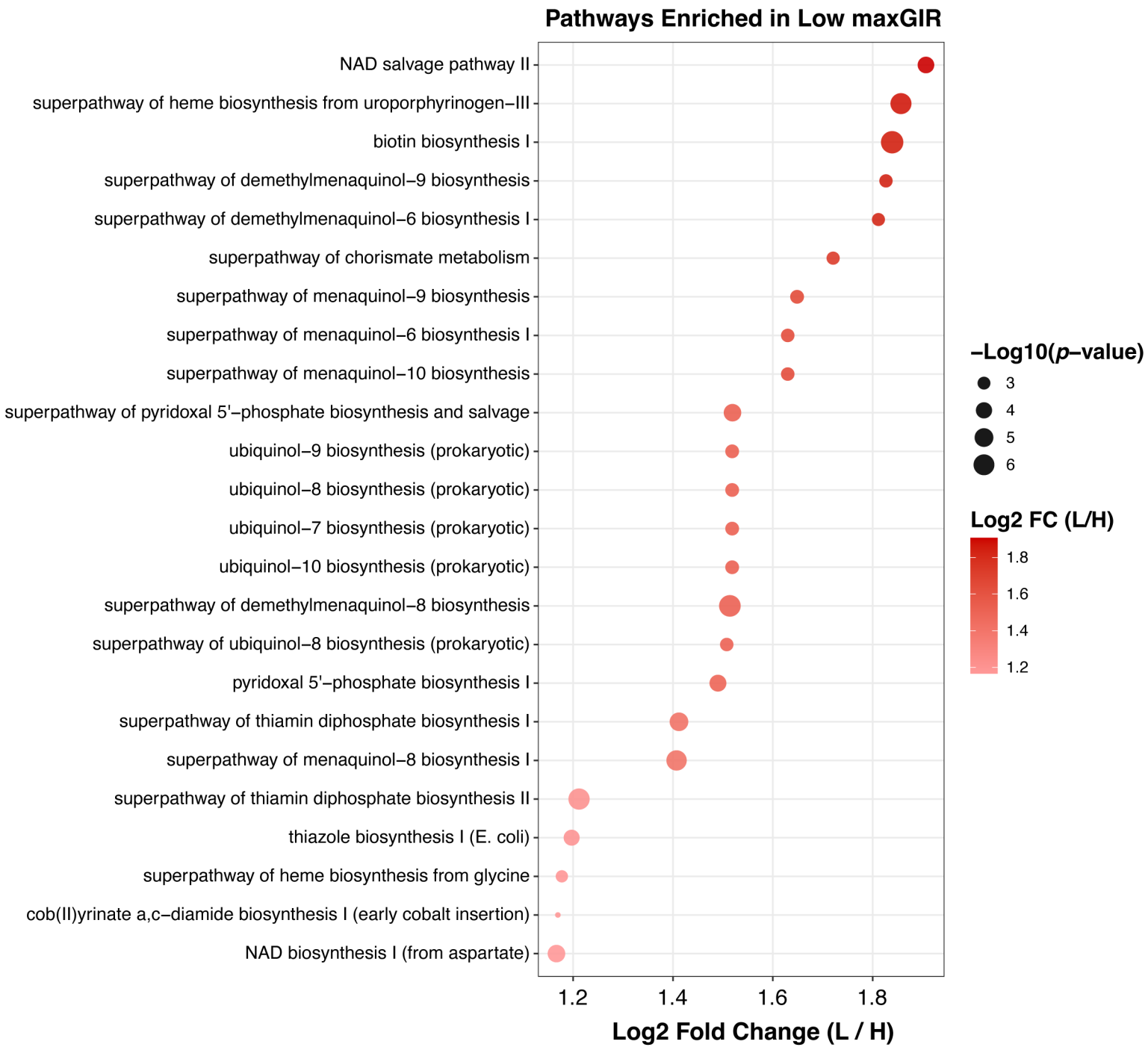
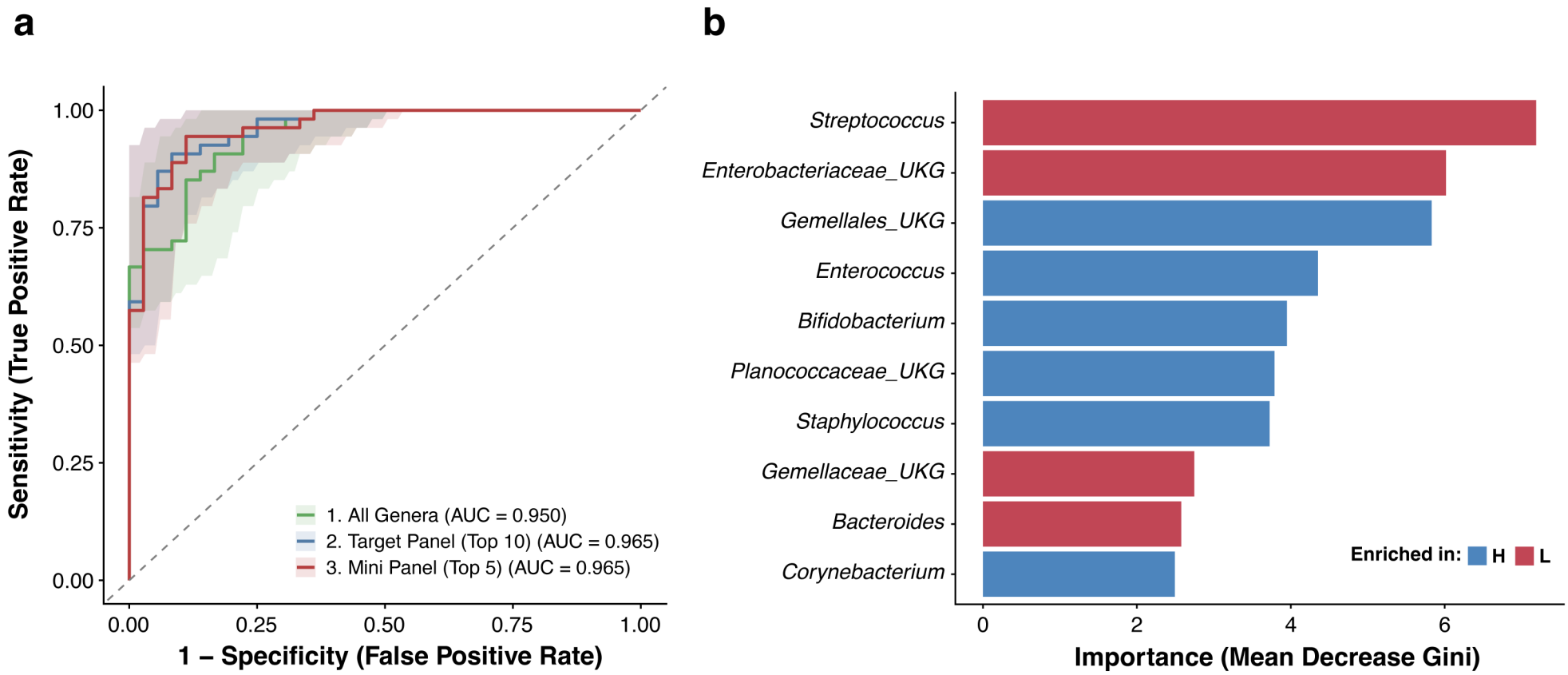

Pathways Enriched in Low maxGIR
NAD salvage pathway II
superpathway of heme biosynthesis from uroporphyrinogen–III
biotin biosynthesis I
superpathway of demethylmenaquinol–9 biosynthesis
superpathway of demethylmenaquinol–6 biosynthesis I
superpathway of chorismate metabolism
superpathway of menaquinol–9 biosynthesis
superpathway of menaquinol–6 biosynthesis I
superpathway of menaquinol–10 biosynthesis
superpathway of pyridoxal 5'–phosphate biosynthesis and salvage
ubiquinol–9 biosynthesis (prokaryotic)
ubiquinol–8 biosynthesis (prokaryotic)
ubiquinol–7 biosynthesis (prokaryotic)
ubiquinol–10 biosynthesis (prokaryotic)
superpathway of demethylmenaquinol–8 biosynthesis
superpathway of ubiquinol–8 biosynthesis (prokaryotic)
pyridoxal 5'–phosphate biosynthesis I
superpathway of thiamin diphosphate biosynthesis I
superpathway of menaquinol–8 biosynthesis I
superpathway of thiamin diphosphate biosynthesis II
thiazole biosynthesis I (E. coli)
superpathway of heme biosynthesis from glycine
cob(II)yrinate a,c–diamide biosynthesis I (early cobalt insertion)
NAD biosynthesis I (from aspartate)
1.2
1.4
1.6
1.8
Log2 Fold Change (L / H)
–Log10(p–value)
3
4
5
6
Log2 FC (L/H)
1.8
1.6
1.4
1.2

Fig. 5


a
b
Sensitivity (True Positive Rate)
1 – Specificity (False Positive Rate)
1. All Genera (AUC = 0.950)
2. Target Panel (Top 10) (AUC = 0.965)
3. Mini Panel (Top 5) (AUC = 0.965)
Streptococcus
Enterobacteriaceae_UKG
Gemellales_UKG
Enterococcus
Bifidobacterium
Planococcaceae_UKG
Staphylococcus
Gemellaceae_UKG
Bacteroides
Corynebacterium
Enriched in: H L
Importance (Mean Decrease Gini)

Supplementary Files

This is a list of supplementary files associated with this preprint. Click to download.

- Table1.Clinicalcharacteristicsoftheneonates..docx
- supp.figure.docx